CONTROL LOAD ENVELOPE SHAPING BY LIVE TWIST

F. J. Tarzanin, Jr.
Senior Engineer, Boeing Vertol Company, Philadelphia, PA

P. H. Mirick
Aerospace Engineer, Eustis Directorate, USAAMRDL, Ft. Eustis, VA

Abstract

For flight conditions at high blade loadings or airspeeds, the rotor control system experiences a rapid load growth, resulting from retreating blade stall. These loads frequently grow so large that the aircraft flight envelope is restricted long before the aircraft power limit is reached. A theoretical study of one flight condition and a limited model test have shown that blade torsional flexibility plays a major role in determining the magnitude of these large, stall-induced control loads. Recently, an extensive analytical investigation* was undertaken to determine the effect of changing blade torsional properties over the rotor flight envelope. The results of this study showed that reducing the blade stiffness to introduce more blade live twist** could significantly reduce the large retreating blade control loads. Too much live twist, however, may increase the control loads by introducing a large nose-down advancing blade torsional moment. Still, significant control load reductions can be achieved and the flight envelope can be expanded by increasing live twist to reduce retreating blade stall loads, but not enough to greatly increase advancing blade loads.

Introduction

For any practical helicopter design, the level-flight, steady-state loads should be below the endurance limit (infinite life load) so that sufficient life will be available to absorb the larger maneuver loads. A major design objective is to produce an aircraft with a flight envelope limited by aircraft power and not by structural limits Frequently, however, the operational flight envelope is limited by a rapid growth of stall-induced control loads that exceed the endurance limit. Therefore, the flight envelope is limited by control loads, and the available power cannot be fully utilized.

The rapid control load growth is attributed to stall flutter which is a consequence of high angles of attack and resulting blade stall. Visual confirmation of the large stall loads can be found in pitchlink or blade torsional gage waveforms on which characteristic stall spikes appear in the fourth quadrant of the blade azimuth. These high loads result from an aeroelastic, self-excited pitch motion in conjunction with repeated submersion of a large portion of the rotor blade in and out of stall.

An aeroelastic rotor analysis program[1] was developed, using unsteady aerodynamic theory that could preduct the large stall-induced control loads. Limited analytical studies of a single flight condition, using this program[2] and another study by Sikorsky Aircraft[3], indicated that modifications to the blade torsional properties could significantly reduce the stall-induced control loads. These encouraging theoretical results led to a model test[3] to verify the control load reduction. The test results showed that, by reducing the blade torsional natural frequency from 5.65 to 3 per rev, the model stall flutter torsion spike was reduced 73 percent, giving a first verification of the analytical trend.

Next, an extensive study was undertaken to explore the impact of modified blade torsional properties on blade torsional loads over the flight envelope. The study had two major parts--the first part compared model test results of blades with different torsional properties with analytical results to evaluate the analysis; while the second part analytically explored the variation of control loads for flight conditions of hover and 125, 150, and 175 knots with blade loadings (C_T/σ) from 0.05 to 0.18. This paper summarizes the results of this study.

Theory and Test Comparison

For useful analytical results, confidence in the theory must be established to show that the fundamental phenomena are properly accounted for. The aeroelastic rotor analysis has been successfully correlated with control loads obtained from full-scale CH-47C flight data for both stalled and unstalled conditions. Additional correlation with the model rotors

* Work performed under Contract DAAJ02-72-C-0093, Investigation of Torsional Natural Frequency on Stall-Induced Dynamic Loading, by The Boeing Vertol Company, U. S. Army Air Mobility Researc and Development Laboratory (USAAMRDL).

** Live twist is the steady and vibratory elastic pitch deflection that results from blade torsional loads.

test was performed to further evaluate the analysis.

The model test used three six-foot diameter rotor sets. Each rotor set had three articulated blades with identical airfoil and planform, but each set had a different torsional natural frequency. The first set of blades had a torsional natural frequency of 4.25 per rev and was constructed of fiberglass, using conventional crossply torsion wrap. The second set of blades had mass properties similar to the first blade set, but had a torsional natural frequency of 3.0 per rev. These blades were constructed with fiberglass, using a uniply torsion wrap which substantially reduced the blade torsional stiffness. The third set of blades had a torsional natural frequency of 5.65 per rev and was constructed of carbon composite. Although the carbon blades were not significantly stiffer than the first set of blades, they had significantly lower torsional inertia which accounted for the higher torsional natural frequency.

A number of runs were made for each rotor set at full-scale tip speeds and an advance ratio of 0.3. Due to the difference in torsional properties, the blade live twist of each rotor set was different, resulting in propulsive force and thrust differences for identical collective, cyclic, and shaft angle. One run for each rotor set was selected such that the rotors would have similar propulsive force variations with thrust. From each of these runs, five test points were selected which covered the range of available blade loading (C_T/σ) and which provided at least one flight condition below stall, one condition in transition, and two stalled conditions. A detailed description of the test conditions and all the model blade physical properties are given in Reference 4.

The variation of test and analytical blade torsion amplitude with blade loading (C_T/σ) is shown in Figures 1, 2, and 3 for the low stiffness, standard reference, and carbon blades, respectively. Each blade was instrumented to record blade torsion data. Due to gauge failures, only two gauges on the standard reference blades and only one gauge on the carbon blades were operational. In general, the analysis correctly predicts the trend of blade torsional load amplitude with blade loading for both stalled and unstalled flight conditions. The predicted stall inception agrees well with test for the low stiffness blade. For the standard reference blade and the carbon blade, stall inception is predicted about 0.01 C_T/σ too early (see Figures 2 and 3). The analysis predicts approximately the correct torsional load growth rate in stall; but, because the stall inception is predicted early, the

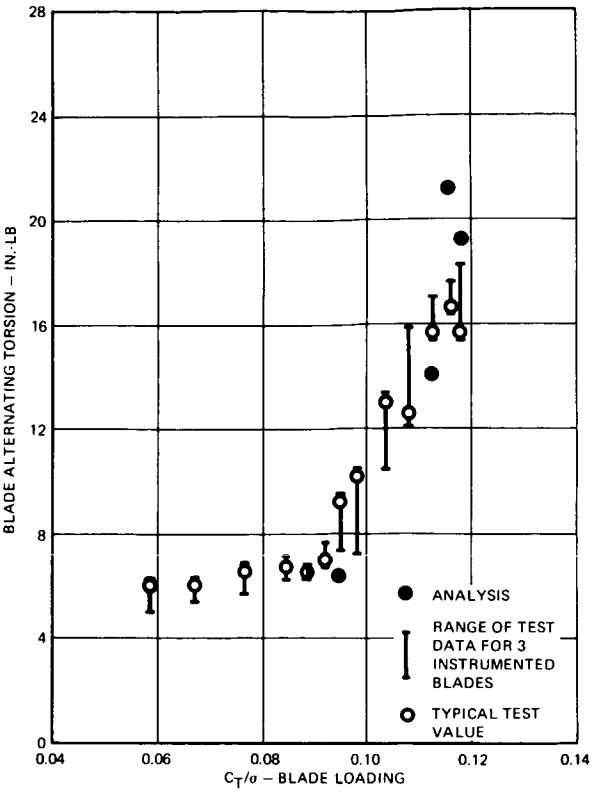

Figure 1. Comparison of Measured and Calculated Blade Torsion Amplitude for the Low Stiffness Blade (3 per rev).

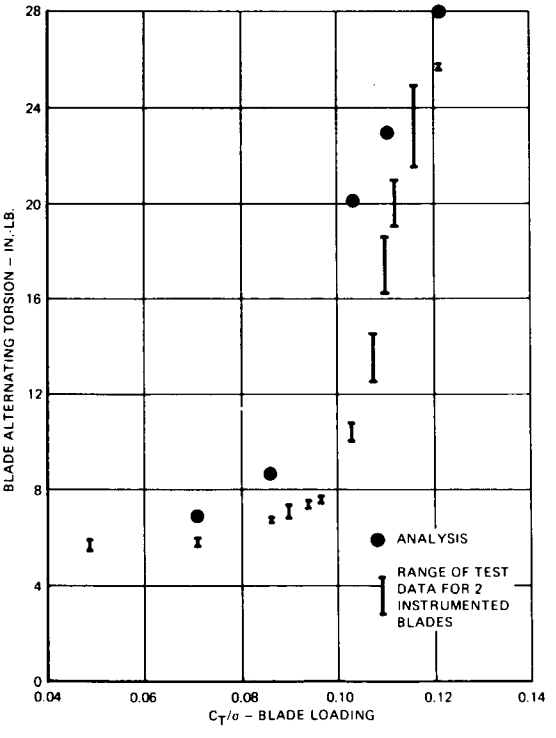

Figure 2. Comparison of Measured and Calculated Blade Torsion Amplitude for the Standard Blade (4.25 per rev).

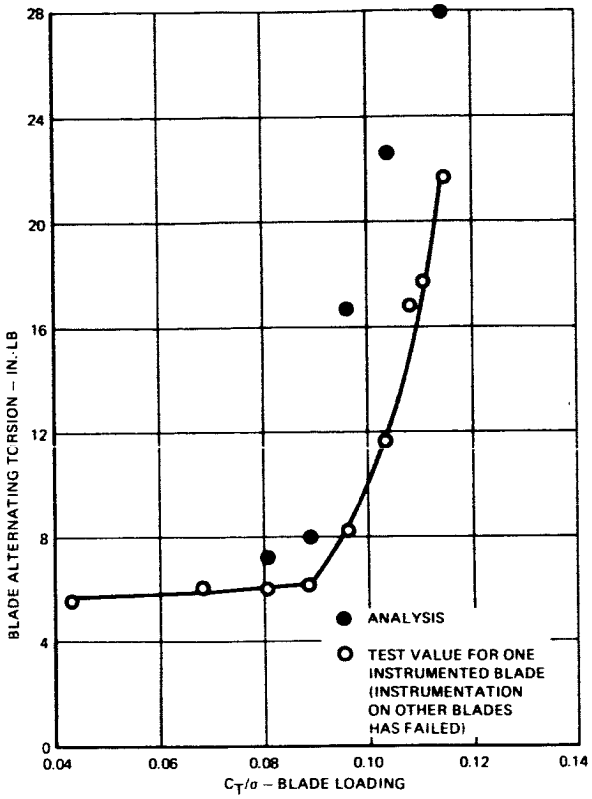

Figure 3. Comparison of Measured and Calculated Blade Torsion Amplitude for the Carbon Blade (5.65 per rev).

stall loads are overpredicted for the two stiffer blades.

A number of possible explanations for the analytical overprediction are discussed in Reference 4. The two most likely explanations are first, questionable model blade physical properties (possible 0.02 chord error in the carbon blade center of gravity, 0.06 chord error in the standard blade shear center, and -0.07 chord error in the carbon blade shear center) secondly, the unsteady aerodynamic plunging representation is inadequate (a lack of cyclic pitch led to model blade flapping of 12 , the theory may be overly sensitive to these large plunging velocities).

Even though correlation is not as good as desired, it is clear that the analysis predicts the large stall-induced control load increase (stall flutter), approximates the control load increase with increasing rotor thrust, and defines the proper load trend for changes in blade torsional properties. These results are sufficient to provide a degree of confidence in the theoretical trends, indicating that the qualitative results of the flight envelope investigation are meaningful.

Analytical Investigation of Stall-Induced Dynamic Loading

The analysis and test of Reference 2 showed that changes in blade torsional property can change the stall-induced control loads. For this discovery to have a practical application, it must be shown that realistic changes in the blade torsional properties will lead to a significant reduction in the large stall-induced control loads throughout the flight envelope. To determine the variation of control loads over the flight envelope, an extensive analytical study was performed. The aircraft used for this study was a single-rotor helicopter with CH-47C blades. A 20.1 square-foot frontal area was assumed for the fuselage and a tail rotor sufficient for trim purposes was added. The main rotor consisted of three articulated 30-foot radius blades with a constant chord of 25.25 inches. The blade cross-section is a cambered 23010 airfoil with 9.137 degrees of linear twist along the blade span.

To perform this study, blade torsional properties were modified by changing blade torsional stiffness (GJ), changing control system stiffness, and changing blade pitch inertia. Using the CH-47C blade's torsional natural frequency of 5.2 per rev as a baseline, the frequencies were adjusted from 3 per rev to 7 per rev.

Natural frequencies of 3 rev, 4 rev, and 7 rev were obtained by multiplying the torsional stiffness distributions by 0.25, 0.5 and 3.3, respectively. A control system stiffness of 1650 pounds per inch generated a frequency of 3 per rev; 11,850 pounds per inch was used for the basic blade, and an infinite stiffness produced a 6 per rev frequency. Pitch inertia changes resulted in blades with frequencies of 3, 4 and 7 per rev due to scaling the pitch inertia by factors of 3.08, 1.7 and 0.55, respectively. All changes were made by only varying the blade properties indicated, while holding all other parameters at the nominal CH-47C values.

Figure 4 shows the relationship between pitch-link load amplitude and torsional frequency (3 per rev to 7 per rev) at an airspeed of 125 knots and a blade loading of 0.115 for the three methods of varying frequency. Each method produced approximately the same trend of increasing pitch-link loads with increasing torsional natural frequency. Figure 5 illustrates the variation of pitchlink load amplitude with natural frequency at 150 knots airspeed and blade loadings of 0.115. For both airspeeds, the variation in torsional stiffness leads to larger changes in pitch-link loads, than do changes in control stiffness or pitch inertia.

Since blade torsional stiffness changes resulted in the largest change in control load and the lowest loads, the effect of blade torsional stiffness changes will be

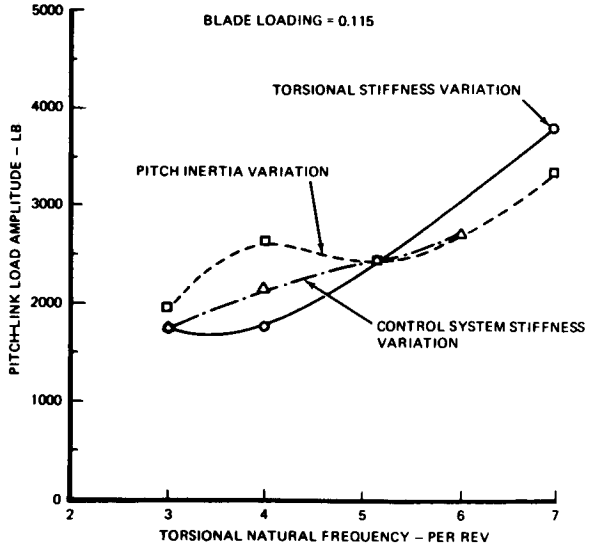

Figure 4. Variation of Pitch-Link Load Amplitude with Natural Frequency at 125 Knots.

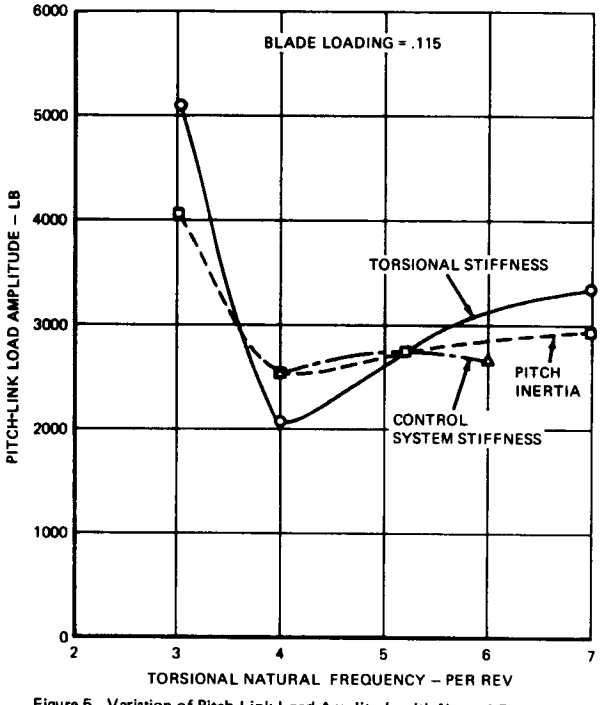

Figure 5. Variation of Pitch-Link Load Amplitude with Natural Frequency at 150 Knots.

explored in greater depth. It is apparent from these results that it is not the reduced torsional frequency alone that reduces pitch-link loads, but also the increase in blade live twist, resulting from reduced torsional stiffness.

Four blades with different torsional natural frequencies (i.e., 3 per rev, 4 per rev, 5.17 per rev and 7 per rev) were analyzed for 24 flight conditions to investigate the interactive effects of torsional stiffness, blade loading (C_T/σ), and airspeed. The airspeeds ranged from hover to 175 knots and blade loading from 0.05 to 0.018.

Hover

Figure 6 shows the variation of pitch-link load amplitude with blade loading for four sets of rotor blades. One degree of cyclic pitch was used to provide some means of introducing a cyclic load variation. If this were not done, the analysis would predict only steady loads. At blade loadings of 0.115 and 0.12 the pitch-link load has a 1-per-rev waveform with an amplitude of about 100 pounds for all four blades. These loads represent an unstalled condition, and there is virtually no load variation with blade loading or torsional natural frequency. At a blade loading of 0.15, the loads increase to between 200 pounds and 300 pounds, with the 3 per rev and 4 per rev blades having the lowest load. At this condition, the rotor power is around 4000 horsepower which is well beyond the available rotor power.

At a blade loading of 0.165, the pitch-link load for the 3 per rev blade increases sharply to 1000 pounds. The major portion of this load is a 950 pound, 8-per-rev component. Since the blade torsional natural frequency is 3 per rev, it was surprising to observe that there was little 3-per-rev load and a very large 8-per-rev load. Further examination revealed that the blade second torsional natural frequency is almost exactly 8 per rev, explaining the source of the large load. It is not known why the torsionally soft blade prefers to oscillate in its second mode. Further investigation is necessary.

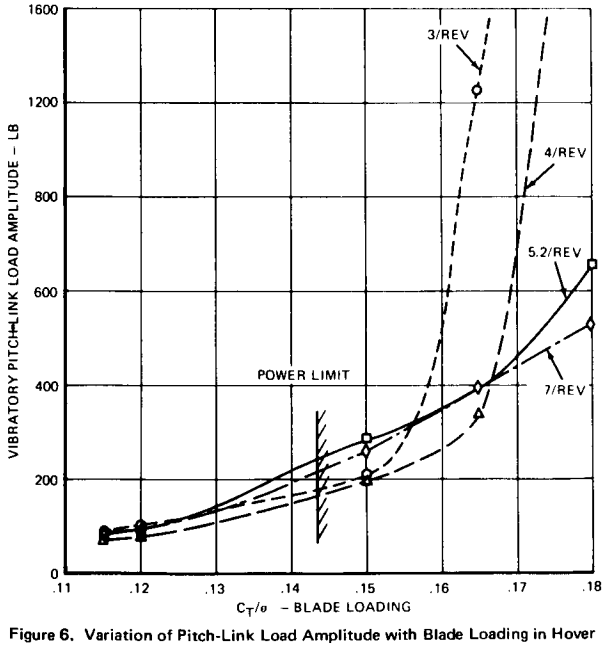

Figure 6. Variation of Pitch-Link Load Amplitude with Blade Loading in Hover for One Degree of Cyclic Pitch.

The 4-per-rev blade, at the same flight condition, has a pitch-link load of 340 pounds which is the lowest of the four blades. The 5.2-per-rev and 7-per-rev blades had approximately the same load at about 400 pounds. The required rotor power for all blades is approximately 5000 horsepower which is 66-percent more than the available rotor power of a CH-47C rotor. Since the required power is so high, results at this (0.165) and higher blade loadings probably have no practical application.

At a blade loading of 0.18, the 3 per rev blade pitch-link load increases to 4500 pounds, with the 8-per-rev component again providing the largest load. The 4-per-rev blade also shows a large load increase, reaching a load of about 4000 pounds. However, this blade's large torsional loads occurred at the first torsional natural frequency (3600 pounds at 4 per rev). The 5.2-per-rev blade has a load of 650 pounds and the 7-per-rev blade load is 540 pounds. At this condition, the loads reduce with increasing torsional frequency. The required rotor power for this flight condition is over twice the available power, indicating that rotor stall has reached a larger portion of the blade.

These results indicate that in hover, increased torsional frequency (i.e., torsional stiffness) delays the inception of stall flutter. This conclusion generally agrees with propeller experience. However, the large power required at a blade loading of 0.16 (i.e., 50 percent above available power) implies that this flight condition and higher blade loadings do not apply to current aircraft. If current power to rotor solidity ratios are therefore used, there is very little difference between the torsional loads of the four blades up to reasonable blade loadings (for this discussion, approximately 0.15 blade loading).

125 Knots

The variations of pitch-link loads with blade loading for each of the four different torsional frequency blades are shown in Figure 7 for an airspeed of 125 knots. The basic blade (with a torsional natural frequency of 5.2 per rev) pitch-link load increases slowly with increasing blade loading up to a value of 0.10. In this region, the pitch-link load waveform is predominantly 1 per rev (see Figure 8) and the loads are classified as unstalled (even though some stall is present). Stall inception occurs at a blade loading of about 0.103. The stall inception represents the flight condition in which the control loads begin to exhibit the rapid increase, due to blade stall. In this region, the pitch-link load waveform has a large, high-frequency torsional load component which generally appears between an azimuth position of 270 degrees to 60 degrees and usually determines the load amplitude as shown in Figure 9. The stalled pitch-link load continues to rise to 2650 pounds at a blade loading of 0.11. Increasing the blade loading beyond this point results in a load reduction. This reversal of the load trend may at first appear surprising, but it has been observed in model data (see Figure 1) and full-scale results (see Figure 10).

The 7-per-rev blade has generally the same pitch-link load trend, with blade loading as the basic blade. There is an unstalled load region up to a blade loading of 0.09 (with a typical waveform given in Figure 8), a stalled load region typified by a large load increase with blade loading (with a typical stalled waveform at a blade loading of 0.10 as shown in Figure 8), and a load reversal at a blade loading of 0.11. However, as far as control loads are concerned, the 7-per-rev blade is significantly worse than the basic blade. In the unstalled region, the loads are about the same; in stall the 7-per-rev blade loads are 65-percent larger. Stall inception occurs at a blade loading of about 0.095 which is 0.008 before the basic blade.

The 4-per-rev blade has a significantly different pitch-link load trend with increasing blade loading than the two blades

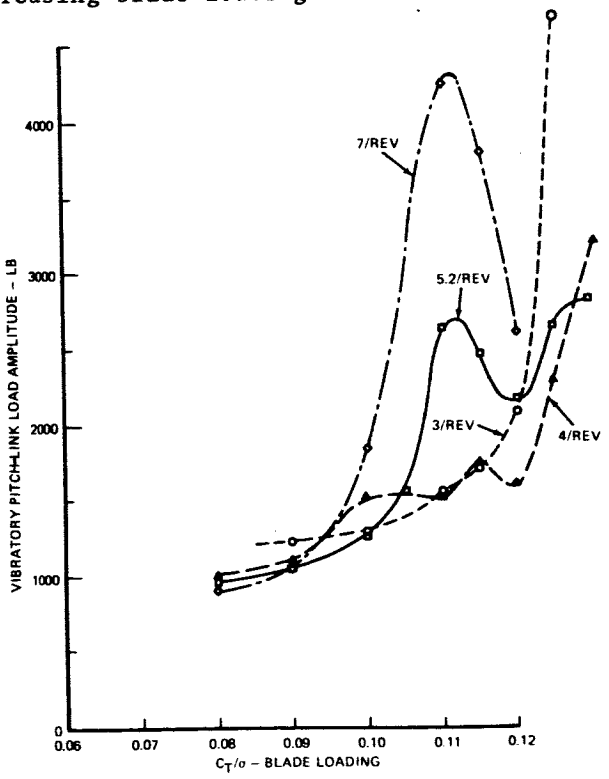

Figure 7. Variation of Pitch-Link Load Amplitude with Blade Loading at 125 Knots.

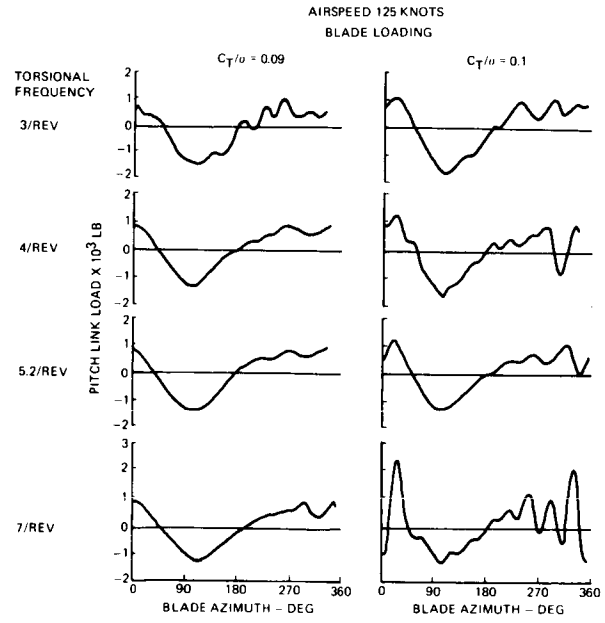

Figure 8. Pitch-Link Load Waveforms for 125 Knots, at Blade Loadings of 0.09 and 0.10.

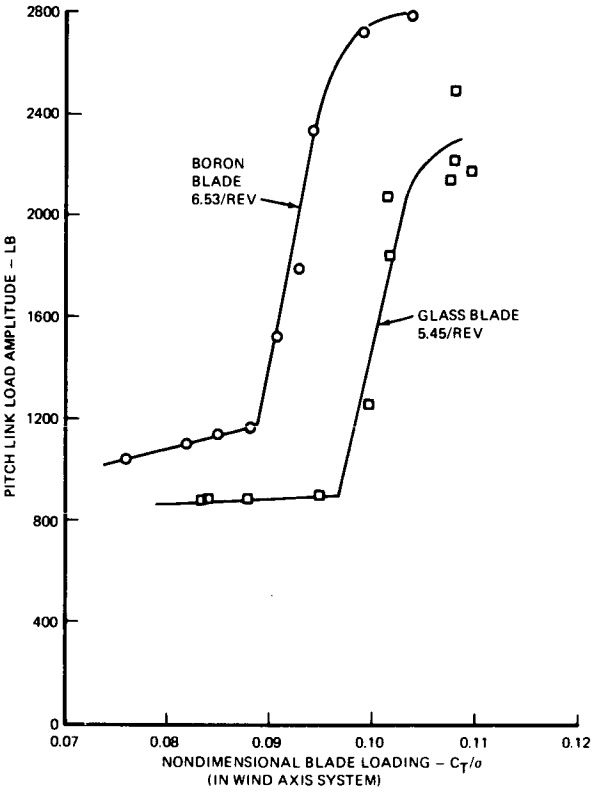

Figure 10. CH-47C Advanced-Geometry Blade Flight Test Data at an Advance Ratio of 0.2.

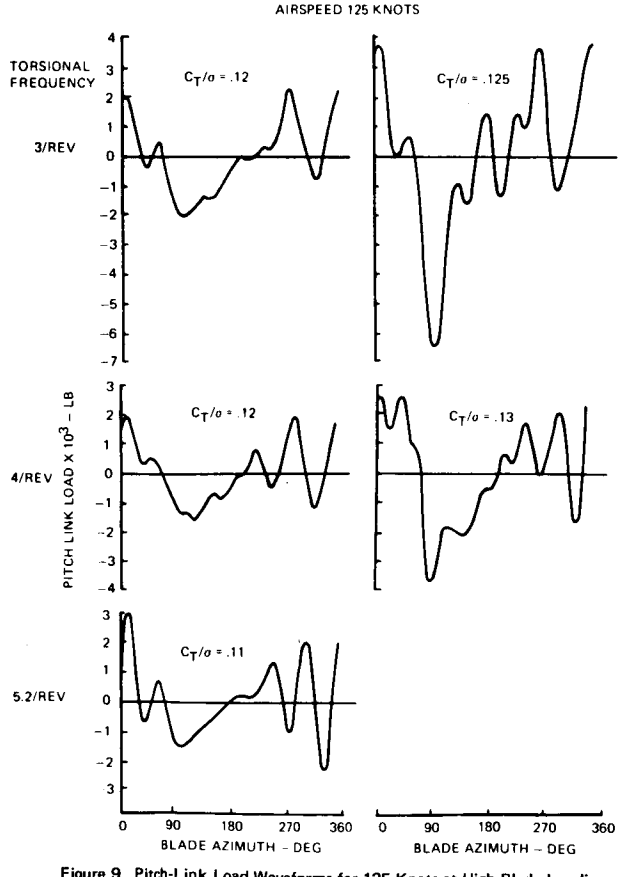

Figure 9. Pitch-Link Load Waveforms for 125-Knots at High Blade Loadings.

previously discussed. While there is the typical unstalled region with little load growth up to a blade loading of 0.09 (a typical unstalled waveform is given in Figure 8), there is an irregular, but moderate, load growth between 0.09 and 0.12. At a blade loading of 0.12, the torsion load is only 1641 pounds and the waveform just attains a fully stalled characteristic (see Figure 9). There is a large load increase (1360 in-lbs) as the blade loading increases from 0.12 to 0.13. Examining the 0.13 pitch-link load waveform (see Figure 9) shows that the large load is not caused by stall flutter; instead, it is due to a large nose-down moment generated by the advancing blade combined with moderate stall spikes.

The 3-per-rev blade has a load trend similar to the 4-per-rev blade. The unstalled load region extends to a blade loading of 0.115, and a typical unstalled waveform is given in Figure 8. Even at a blade loading of 0.12, the pitch-link load waveform does not show a fully stalled waveform (see Figure 9). However, at 0.125, the pitch-link load increases by 150 percent to 5273 pounds, by far the largest load of any blade. The waveform at 0.125 (see Figure 9) shows large stall spikes with an amplitude of 2500 pounds; however, the large load increase is due to

a 5000 pound load at 90° azimuth which results from a large nose-down pitching moment. The load growth is so large at this condition that it may represent the lower boundary of an instability.

It is clear from these results that stall inception occurs earlier as the blade torsional frequency is increased. Further, the maximum retreating blade stall-induced pitch-link loads are larger for blades with higher torsional frequencies (i.e., the 7-per-rev blade has the largest stall-induced loads).

The CH-47C flight test data substantiating the conclusion that stall inception occurs at higher blade loadings as blade frequency is decreased. Figure 10 shows the results of a CH-47C advanced-geometry blade flight test for aft rotor blades with a boron filament spar and a fiberglass spar at an advance ratio of 0.2. The glass blade has a stall inception delay of 0.0085, due to reducing the torsional frequency from 6.53 per rev to 5.45 per rev. The single-rotor study results show a stall delay of 0.008 for reducing the torsional frequency from 7 per rev to 5.2 per rev at an advance ratio of 0.3.

The large advancing blade loads experienced by the 3-per-rev and 4-per-rev blades, beyond a blade loading of 0.12, are not due to the stall-flutter phenomenon which results from retreating blade stall and unstall cycles. This load is associated with the negative lift on the advancing blade tip and appears to be a divergence-like phenomenon. Large, negative tip lift causes the blade to bend tip down; the high tip drag coupled with the flap deflection causes a nose-down moment. The moment causes elastic nose-down pitch which leads to more negative lift, resulting eventually in even larger loads.

150 Knots

At 150 knots (see Figure 11), the basic CH-47C blade has an unstalled load region up to about 0.08 which is typified by a slow increase of pitch-link load with blade loading and a predominantly 1-per-rev waveform. In the region between 0.08 and 0.1, a different load trend is observed. The load increases gradually from 1500 to 2000 pounds, but at a faster rate than the sub-stall load growth, and the waveforms show significant evidence of stall spikes for the retreating blade (see Figure 12). Stall inception (i.e., rapid load growth) appears to occur around 0.103, reaching maximum load near 0.11 (see Figure 12). The load drops at a blade loading of 0.115, showing a load reversal as observed at 125 knots.

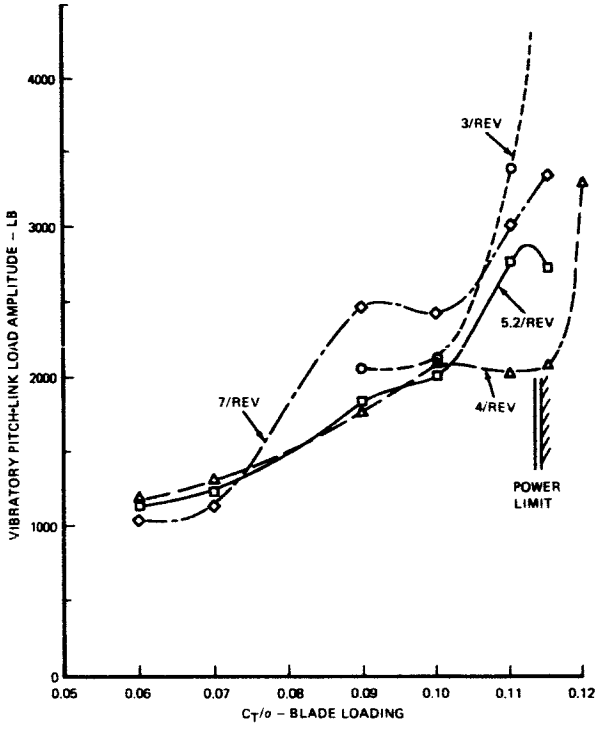

Figure 11. Variation of Pitch-Link Load Amplitude with Blade Loading at 150 Knots.

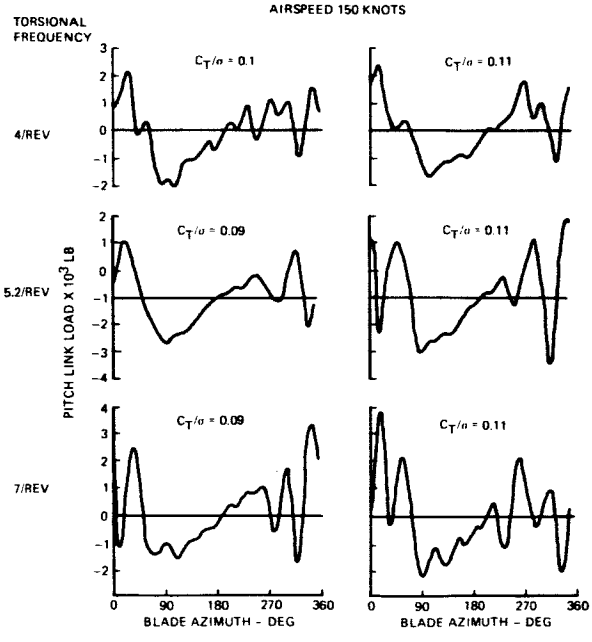

Figure 12. Pitch-Link Load Waveforms at 150 Knots for Blade Loadings of 0.09 to 0.11.

The 7-per-rev blade shows a similar load trend with blade loading as the basic blade, but with significantly larger stall loads. The unstall loads occur up to 0.07. Stall inception occurs at approximately 0.075, reaching a fully stalled waveform at 0.09 (see Figure 12). The loads level out at 0.10, reach a second stall inception near 0.105, and the load begins to grow again. Examining the pitch-link load waveform at 0.11 (see Figure 12) shows that the load increase is due to a large stall spike occurring in the 0 to 50-degree azimuth region, not to retreating blade stall spikes.

With an expected unstalled waveform the 4-per-rev blade has a typical unstalled control load growth up to a blade loading of about 0.09. Between 0.09 and 0.115, there is an irregular load growth. In this region, the waveforms show evidence of retreating blade stall (see Figure 12), but no large load increase. At a blade loading of 0.11, the torsion load is 2100 pounds and the waveform just attains a fully stalled characteristic (see Figure 12). There is a 1230-pound load increase as the blade loading increases from 0.115 to 0.12. Examining the 0.12 pitch-link load waveform (see Figure 13) shows that the large load increase is caused by a large, advancing-blade nose-down spike combined with retreating blade stall spikes.

The 3-per-rev blade shows a reasonable pitch-link load through a blade loading of 0.11. However, at 0.115, the blade is apparently unstable since the loads have grown so large that the blade would probably fail. The pitch-link load waveform at 0.11 (see Figure 13) contains relatively small retreating-blade, stall-induced spikes. There is, however, a large compression load for the advancing blade at 90 degrees blade azimuth. By examining the pitch link load waveform for the unstable flight condition, it appears that the blade divergence involves a large advancing blade compression load that continually increases with each rotor revolution.

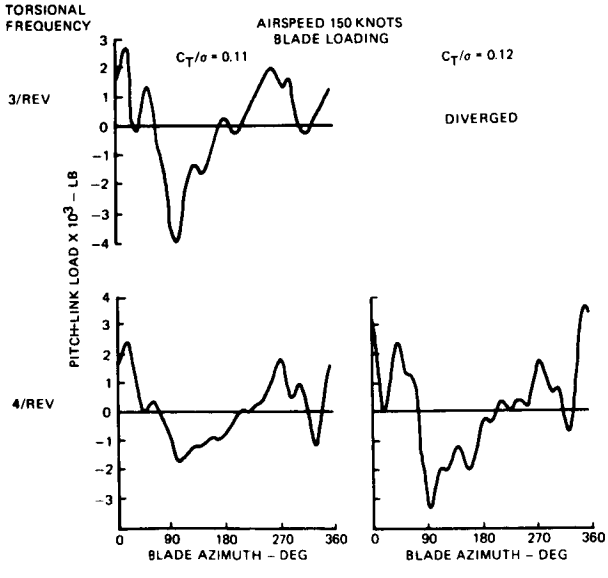

Figure 13. Pitch-Link Load Waveforms at 150 Knots for the 3-per-rev and 4-per-rev Blades at High Blade Loadings.

The 3-per-rev blade is experiencing an additional problem which is not apparent by simply observing the load trend. For all the load conditions calculated at 150 knots, the required power exceeds the available power. Apparently, the blade is experiencing so much live twist that there is a significant increase in rotor drag. The other blades, by contrast, exceed the available power only at a blade loading of 0.115. It is, therefore, obvious that the 3-per-rev blade is not an acceptable configuration for the 150-knot flight condition.

175 Knots

At 175 knots (see Figure 14), the basic blade pitch-link load trend shows unstalled loads continuing to a blade loading of 0.07 and stall inception occurring about 0.075. The stalled load increases with a moderate growth rate up to 0.09. Figure 15 illustrates the pitch-link load waveform at 0.09, showing the retreating blade stall spikes and a large nose-down load at 90 degrees azimuth. Beyond a blade loading of 0.09, the load does not reverse as it does for previous airspeeds (even though the retreating blade stall spike is significantly reduced at a blade loading of 0.11 as shown in Figure 15). Instead, the load continues to increase at about one half the previous growth rate, due to an increasingly large nose-down load at 90 degrees azimuth.

The 7-per-rev blade pitch-link load trend is almost identical with the basic blade trend up to 0.09. As Figure 15 shows, the waveform exhibits typical high-frequency stall spikes. The torsion load shows a slight load reversal beyond 0.09, but then resumes the load increase at the typical stalled load growth rate. The load growth at 0.11 is due to a combination of a large stall spike at around 30 degrees azimuth and an increasing nose-down load at 90 degrees azimuth (see Figure 15).

The 4-per-rev blade has a typical substall load growth up to 0.07 and generally follows the load trend of the 7-per-rev blade and the basic blade up to 0.08. Beyond this point, the load growth rate drops significantly. At a blade loading of 0.09, the pitch link load is 500 pounds

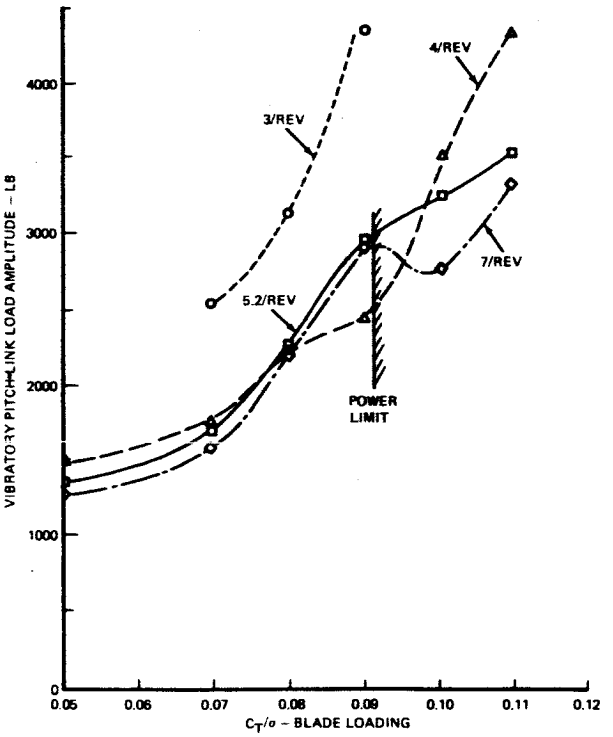

Figure 14. Variation of Pitch-Link Load Amplitude with Blade Loading at 175 Knots.

below the other two blades. Also 0.09, the pitch-link load waveform shows little evidence of retreating blade stall (see Figure 15), but does show that the major component of the load results from a nose-down moment at 90 degrees blade azimuth. Beyond this point, the load growth rate increases sharply from 2500 pounds at 0.09 to 4200 pounds at 0.11.

The 3-per-rev blade is not seriously considered at this airspeed. The loads are 1500 pounds beyond any of the other blades, and an advancing blade instability is apparent at a blade loading of 0.09. Further, the required rotor power exceeds the available CH-47C power for all 175-knot flight conditions examined.

Examining the 175-knot pitch-link load waveforms at a blade loading of 0.11 clearly shows that all four blades experience increased advancing-blade compression loads when compared to the 150-knot waveforms (compare Figures 12 and 14). The 7-per-rev blade shows a 1300-pound advancing-blade load increase for the 25-knot airspeed increase. The basic 5.2-per-rev blade load increase is 2200 pounds, the 4-per-rev blade load increase is 3500 pounds, and the 3-per-rev blade has diverged. Therefore, the blades experience advancing blade load problems which are intensified as airspeed is increased and blade torsional stiffness is reduced.

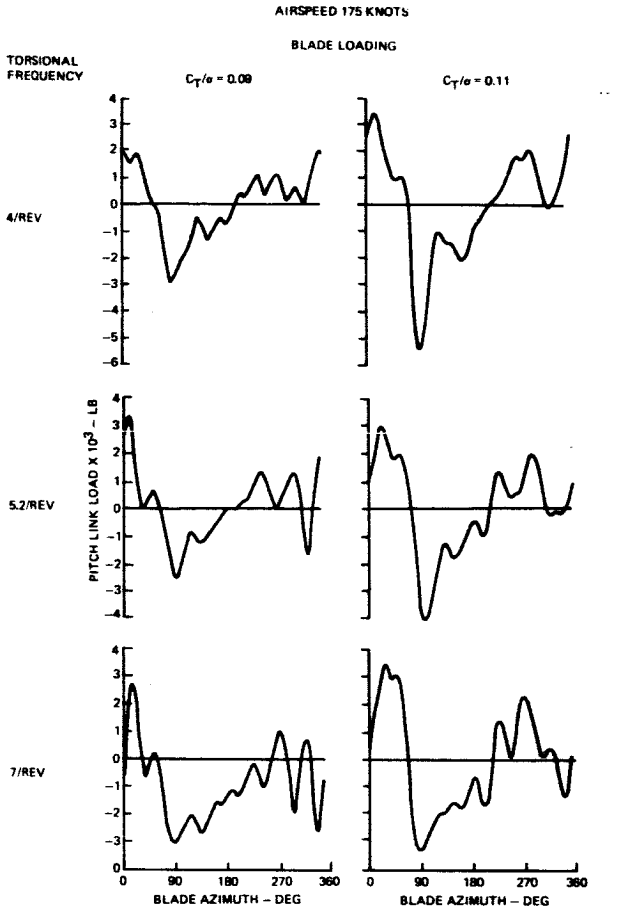

Figure 15. Pitch-Link Load Waveforms for 175 Knots at Blade Loadings of 0.09 and 0.11.

When comparing the 175-knot results for the 4-per-rev, 5.2-per-rev and 7-per-rev blades, it should be noted that the rotor power limit for a single CH-47C rotor is reached just beyond a blade loading of 0.09. For conditions below lthe power limit, the 4-per-rev blade is slightly better than the others, since the maximum pitch-link load is 500 pounds lower. The three blades appear to have adequate maneuver margin, although the 4-per-rev blade may experience larger maneuver loads.

These results show that a significant reduction of the basic blade control loads can be realized over a considerable range of advance ratios and blade loading and that these reductions lead to a significant extension of the control load-limiting aircraft flight envelope. These results can be summarized by obtaining the flight condition (as a function of C_T/σ and μ) that first experiences a 2500-pound pitch-link load. The 2500-pound load approximates the original pitch-link endurance limit load for the CH-47C control system. These flight conditions lead to a blade loading versus advance ratio envelope for the 2500-pound

pitch-link load or an endurance-limit flight envelope. Figure 16 compares the endurance limit flight envelopes for each of the four different frequency blades investigated.

As Figure 16 shows, the blade with a torsional natural frequency of 4 per rev (dashed line) has the best flight envelope and represents a significant improvement over the basic blade configuration. The 4-per-rev flight envelope has essentially the same shape as the basic blade, but it occurs at a higher blade loading. The basic blade envelope occurs at a blade loading of 0.016 below the 4-per-rev blade at an advance ratio of 0.29. At an advance ratio of 0.38, the basic and 4-per-rev blades are approximately equal; but at an advance ratio of 0.4, the 4-per-rev blade envelope is expanded beyond the basic blade by a blade loading of 0.005.

The 3-per-rev blade (short dashes) shows a different flight envelope. At an advance ratio below 0.29, the 3-per-rev blade reaches the endurance limit at a blade loading of 0.123. However, the 3-per-rev envelope drops sharply with increasing advance ratio and eventually falls below the three other blades at a 0.375 advance ratio. The sharp boundary reduction of this blade at the higher advance ratios is due to the large advancing-blade load growth which eventually becomes an instability.* These instabilities show that the 3-per-rev blade is clearly unacceptable, at least for the current pitch-link-controlled configuration.

The 7-per-rev blade clearly has the poorest flight envelope up to an advance ratio of about 0.37. At the higher advance ratios above 0.35, the 7-per-rev blade has the smallest reduction of blade-loading capability with increasing advance ratio. In this region, the 7-per-rev blade surpasses the 3-per-rev blade at an advance ratio of 0.37, surpasses the basic blade at 0.40, and will probably surpass the 4-per-rev blade around 0.44. Therefore, a torsionally stiff blade may be required to attain a reasonable flight envelope beyond advance ratios of 0.44.

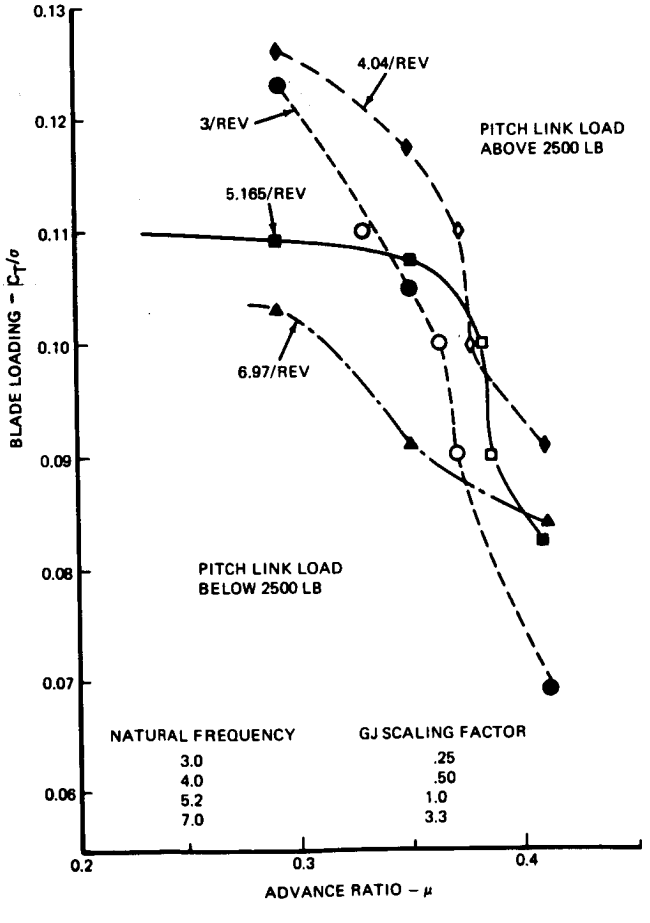

Figure 16. Control Load Endurance Limit Boundaries for Blades with Torsional Natural Frequencies of 3, 4, 5.2 and 7 Per Rev.

Conclusions and Recommendations

The results of the theory-test comparison performed for the 6-foot-diameter model blades and the study of varying torsional properties for the full-scale CH47C size blades have lead to:

1. The theory-test comparison with the 6-foot-diameter model data indicates that the aerolastic rotor analysis reasonably represents the large stall induced control loads, the control load change with blade loading, and the load variation with changes in blade torsional properties. Therefore, the analytical study of the CH47C size blades should provide at least a qualitative evaluation of the control load variation.

2. Changes in control system stiffness, pitch inertia, and blade torsional stiffness vary the large, stall-induced control loads. However, the control load change is not a simple function of torsional natural frequency as previously suspected, since torsional frequency changes, due to varying the blade torsional stiffness, produce control load changes larger than

* It may not be possible for an actual rotor to experience blade divergence. Before large divergence loads result, there is a significant increase in required rotor power. Therefore, a real rotor may simply run out of power and be unable to attain a flight condition for which divergence would occur.

other methods of changing torsional frequency.

3. A blade with a torsional natural frequency of 4 per rev represents a compromise between significantly reducing stall flutter loads, while allowing moderate increases in the advancing blade loads at high speeds. This compromise provides the best endurance limit flight envelope up to an advance ratio of 0.45. Beyond this advance ratio it appears that a torsionally stiff blade will provide a better endurance limit flight envelope.

4. Additional work is required in the following areas.

- A model test program is needed to validate the analytical results over a wide range of flight conditions with remote collective and cyclic pitch to insure trimmed flight.
- Theory improvements are needed to eliminate deficiencies discovered in the theory-test comparison.
- Continue analytical studies to investigate mechanisms of the load generation, maneuver and high-speed load trends and other means for expanding the endurance limit flight envelope.

References

1. F. J. Tarzanin, Jr., PREDICTION OF CONTROL LOADS DUE TO BLADE STALL, 27th Annual National V/STOL Forum of the AHS, Preprint No. 513, May 1971.

2. F. J. Tarzanin, Jr. and R. Gabel, BLADE TORSIONAL TUNING TO MANAGE ROTOR STALL FLUTTER, Presented at the AIAA 2nd Atmospheric Flight Mechanics Conference, AIAA Paper No. 72-958, September 1972.

3. F. O. Carta, L. M. Casellini, P. J. Arcidiacono, H. L. Elman, ANALYTICAL STUDY OF HELICOPTER ROTOR STALL FLUTTER, 26th Annual Forum of the AHS, June 1970. the AHS, June 1970.

4. F. J. Tarzanin, Jr. and J. Ranieri, INVESTIGATION OF TORSIONAL NATURAL FREQUENCY ON STALL-INDUCED DYNAMIC LOADING. Performed under contract DAAJ02-72-C-0092, USAAVLABS TR- (Not yet released).